18. Secondary Eyewall Formation and Eyewall Replacement Cycle Module

Principal Investigators: Hui Christophersen, Robert Rogers, Jason Dunion, Jun Zhang

Collaborators: Jeff Kepert, Kristen Corbosiero, Anthony Didlake, Yuqing Wang, David Nolan and Sergio Abarca

Primary IFEX Goals:

1- Collect observations primarily for mature hurricanes that may undergo a secondary eyewall formation (SEF) and eyewall replacement cycles (ERCs) based on radar, dropsonde, flight-level, Doppler Wind Lidar (DWL), and Coyote PBL measurements;
2- Test utility of new observing platforms (Coyote UAS) and instruments (DWL) in diagnosing physical processes responsible for SEF/ERC, and use data to optimize sampling strategies for improving TC structure predictions in an OSE/OSSE framework;
3- Improve understanding of the dynamic and physical processes that are responsible for SEF/ERC.

Significance & Background:

Secondary eyewall formation (SEF) and eyewall replacement cycles (ERCs) frequently occur during the mature phase of the tropical cyclone (TC) lifecycle. These processes typically result in a halting of the intensification of a TC, and occasionally lead to a temporary weakening as the secondary eyewall becomes the dominant eyewall (Sitkowski et al., 2011). Additionally, they typically lead to a significant broadening of the wind field, increasing the total kinetic energy of the storm and thus the risks from storm surge. Statistical analysis of a 10-year (1997-2007) dataset shows that 77% of major hurricanes (120 knots or higher) in the Atlantic Ocean, 56% in the eastern Pacific, 81% in the western Pacific, and 50% in the Southern Hemisphere underwent at least one ERC (Hawkins and Helveston, 2008). Despite the relative frequency of their occurrence, operational forecasting of SEF/ERCs remains a great challenge, partly since there is no consensus on the mechanisms responsible for SEF or ERC.

There are a wide variety of studies that aim to understand SEF and ERC with different emphases on the internal dynamics and external environmental forcing. The axisymmetric balanced flow, constrained by heat and tangential momentum forcing, generally satisfies gradient wind and hydrostatic balance above the boundary layer (BL) (Abarca and Montgomery, 2013). From the perspective of diabatic forcing, Rozoff et al. (2012) proposed that a sustained azimuthal-mean latent heating outside of the primary eyewall could lead to SEF. This hypothesis was supported by the numerical simulations given by Zhu and Zhu (2014). In a similar sense, diabatic heating/cooling associated with rainbands plays an important role in the structure and intensity change of the storm (Wang 2009; Li et al 2014; Moon and Nolan 2010; Didlake and Houze, 2013a, b) and thus they may also contribute to the SEF/ERC. Didlake and Houze (2013a) proposed that there exists a critical zone where sufficiently high vertical shear of the radial wind can limit the altitude of the convectively induced supergradient flow, leading to low-level convergence in this radial zone and allowing the convection to develop into a secondary eyewall. Corbosiero and Torn (2016) proposed a hypothesis that an increase of convergence induced by the cold pool that formed from convectively-driven downdrafts and low-level radial inflow could enhance rainband convection and lead to SEF. The roles of convective and stratiform heating profiles in rainbands in modifying hurricane structure and intensity, and potentially SEF, is an area of ongoing research.

Montgomery and Kallenbach (1997) proposed that vortex Rossby wave (VRW) interaction with the mean flow may contribute to SEF. VRWs, supported by the radial vorticity gradient outside of the radius of the maximum wind (RMW), propagate from the primary eyewall radially outward until they reach their stagnation radius. At this stagnation radius, inward-moving cyclonic eddy momentum may contribute to SEF. The role of VRWs in SEF is further examined in high-resolution hurricane simulations by Abarca and Corbosiero (2011). Judt and Chen (2010), by contrast, downplayed the importance of VRWs, and

instead attributed the large accumulation of convectively generated PV through eddy heating in the rainband region as an essential factor for SEF.

In contrast to the balanced arguments discussed above, unbalanced dynamics in the BL have also been recognized as an important element in SEF. In this framework, the axisymmetric flow in the BL does not satisfy gradient wind and thermal wind balance. Several studies (Wu et al., 2011; Huang et al., 2012; Abarca and Montgomery, 2013) have pointed out that the precursors of SEF include the broadening of the tangential wind field and the intensification of inflow in the BL, followed by development of supergradient winds and an enhanced horizontal convergence. In-situ observations also demonstrated this existence of supergradient flow (Didlake and Houze, 2011; Bell et al. 2012). Kepert (2013) specifically examined the role of the BL in a balanced vortex framework. He proposed that the BL contributed to the SEF and ERC through a positive feedback mechanism that involves a local enhancement of the radial gradient of vorticity, frictionally forced updraft and convection. Moon et al. (2010) attributed the local vorticity enhancement from processes such as rainband convection.

To test the varying mechanisms proposed to explain SEF and ERC, it is important to obtain kinematic and thermodynamic observations near the eyewall and rainbands. In particular, since most previous analyses focus on azimuthally averaged quantities, it is important to obtain adequate azimuthal and radial sampling both near the primary eyewall and a potentially-developing secondary eyewall. For example, Abarca et al. (2016) pointed out the lack of data particularly at radial distance between 120-200 km in Hurricane Edouard (2014). Additionally, some measure of kinematic and thermodynamic structures along a rainband/developing secondary eyewall can be used to evaluate the along-band structures (Wang 2009; Moon and Nolan 2010; Didlake and Houze 2011, 2013a,b). Observations sampled through this module can be used to evaluate the different proposed mechanisms of SEF and ERC. Data-impact studies on TC analyses and forecasts can also be conducted using the OSSE approach to find optimal sampling strategies for the prediction of SEF/ERC. If this module is flown every 12 h (e.g., in conjunction with the TDR experiment), then the temporal resolution will provide an opportunity to evaluate the importance of the various proposed mechanisms at different stages in the evolution of the secondary eyewall. The dataset from this module eventually will benefit our understanding of the dynamic and physical processes that are responsible for SEF/ERC.

Objectives:

The main objectives of the SEF/ERC module are:

- Perform analyses with sampled observations to examine key factors that are responsible for SEF/ERCs;
- Validate key features linked with different hypotheses of SEF/ERCs using observations;
- Conduct OSE/OSSE studies to optimize sampling strategies for improving SEF/ERC predictions;
- Improve understanding of the dynamic and physical processes of SEF/ERCs.

Hypotheses:

There are many hypotheses for the formation of the secondary eyewall and subsequent ERCs. The sampling strategy proposed here is intended to allow for a testing of as many of these hypotheses as possible. This experiment aims to investigate the following hypotheses:

- Unbalanced boundary layer (BL) spinup paradigm. Processes potentially linked to SEF/ERCs will be examined, including: the generation of supergradient winds in boundary layer, increases in boundary layer inflow, and the emergence of deep convection originating from the boundary layer.
- A feedback mechanism for SEF/ERCs that consists of a local enhancement of the radial vorticity gradient outside of the primary eyewall, with induced frictional updrafts and convection. This

feedback mechanism is linked to a combination of both balanced (e.g. vorticity generation and initiation of upward motion) with unbalanced theory (e.g. the development of enhanced and potentially supergradient flow in the BL).

- Enhanced convergence between cold pools that form from convectively-driven downdrafts and low-level inflow. This convergence invigorates rainband convection that eventually becomes the secondary eyewall.

We note that the above hypotheses place a decidedly different importance on the role of balanced vs. unbalanced processes in SEF/ERC. The first hypothesis states that unbalanced BL processes alone can develop secondary wind maxima without prescribed heat sources and/or inertially constrained swirling flow either within or above the boundary layer. The development of the supergradient winds near the top of the boundary layer coincides with horizontal convergence and the eruption of deep convection out of the BL. The second hypothesis states that the BL process is a 'slave' to the SEF. The local enhancement of the vorticity gradient *causes* the local frictional updraft, while the existence of the supergradient flow is a by-product of this frictional convergence. Though the last tested hypothesis lies in the overall framework of the unbalanced BL spinup paradigm, it emphasizes the role of low moist static energy air within the boundary layer that are associated with the convergence.

Modeling Evaluation:

- Examine the hallmarks of the proposed hypotheses through OSE studies by using the sampled observations
- Further validate proposed hypotheses through a series of OSSE studies

Mission Description:

This module focuses on mature hurricanes (e.g. category 2 or stronger) with a well-defined eye as seen in visible, infrared, and microwave satellite imagery. Sampling can be achieved in combination with the P-3 Doppler Wind Lidar, Coyote UAS and P-3, G-IV or Global Hawk dropsondes. This module can generally be flown in conjunction with TDR Experiment survey patterns, with the addition of either a spiral pattern (pre-SEF) or moat circumnavigation (post-SEF) added onto the survey. The module can also be flown during the TC Diurnal Cycle Experiment and DWL Experiment.

Module Option 1 (PRE-SEF): Mature hurricane that has pronounced rainband activity, and possibly a secondary eyewall forming. Proposed flight pattern (Fig. 18-1) should take place when microwave satellite imagery indicates the presence of asymmetric rainbands occurring in the storm environment.

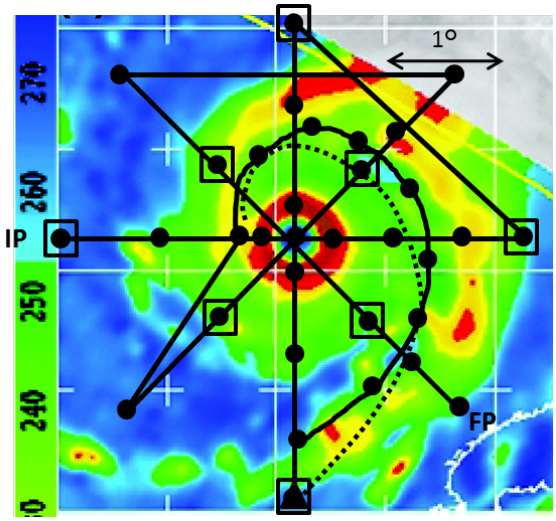

(a)

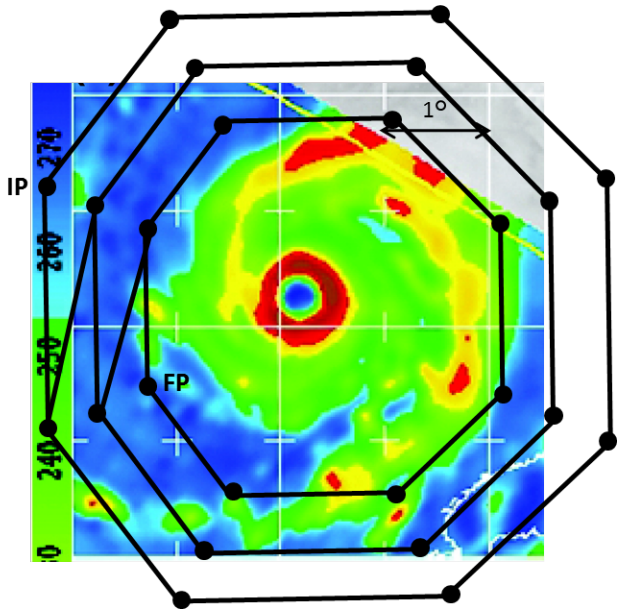

(b)

Figure 18-1*: (a) P-3 Rotating figure-four pattern with Coyote deployed inflow path (dashed line; proposed launch point for Coyote Inflow Module indicated by triangle) overlain on a sample 85 GHz satellite image, showing pre-SEF, to depict features to target. Circles indicate dropsonde locations; open squares indicate AXBT deployment locations. Alternatively, the use of IR sondes would be preferred. This scenario may be combined with DWL Experiment. (b) G-IV circumnavigation pattern.*

- Altitude: 10,000-12,000ft (3-4 km) altitude preferable for P-3
- Expendables: For P-3, deploy dropsondes at all turn and mid-points in Figure 4 survey pattern, first center pass, four locations in primary eyewall, and in middle of rainband precipitation feature. Also release dropsonde at ~50 nm spacing along rainband spiral. If Coyote is available, deploy it following the inflow path where it will collect observations that can be used to calculate BL characteristics outside, within, and inside rainband. For G-IV, release dropsondes at all turn points.
- Pattern: For P-3, fly a combination of a rotated Figure-4 and a rainband spiral along the inside edge of the rainband, within ~5-10 nm of the inner edge of the rainband. Fly the spiral pattern straight and level as long as possible, i.e., keeping aircraft bank angle at a minimum, to minimize loss of radar data due to aircraft banking. Ferry time may preclude the second Figure-4. For G-IV, fly pattern such that the innermost circumnavigation is as close to outer edge of rainband as is safely allowed.

Module Option 2 (POST-SEF): Mature hurricanes that are expected to have a secondary eyewall already formed or are undergoing an ERC. These concentric rings can be easily detected based on radar or microwave satellite imagery. For storms that are already undergoing these ERCs and repeated ERCs are forecast, sampling patterns as indicated in Fig. 18-2 are proposed.

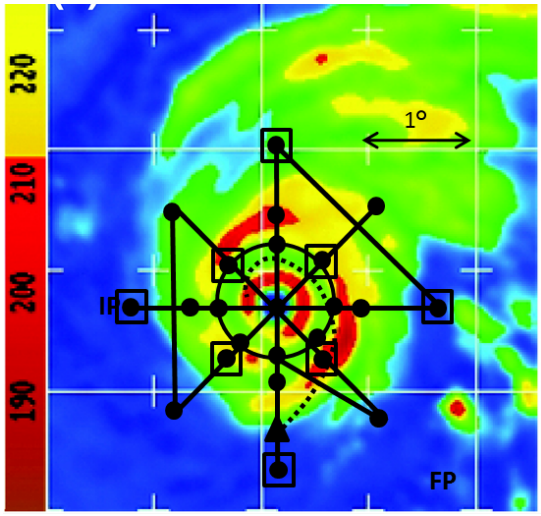

(a)

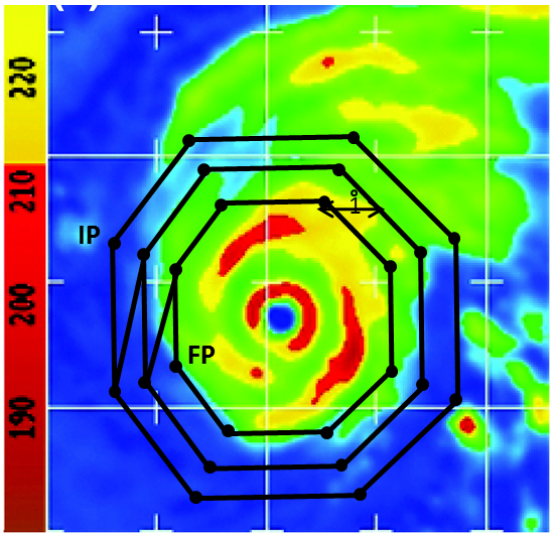

(b)

Figure 18-2*: (a) P-3 Rotating figure-four pattern with Coyote deployed inflow path (dashed line; proposed launch point for Coyote inflow module indicated by triangle) overlain on a sample 85 GHz satellite image, showing post-SEF, to depict features to target. Circles indicate dropsonde locations; open squares indicate AXBT deployment locations. Alternatively, the use of IR sondes would be preferred. This scenario may be combined with DWL module. (b) G-IV circumnavigation pattern.*

- Altitude: 10,000-12,000ft (3-4 km) altitude preferable for P-3
- Expendables: For P-3, Deploy dropsondes at all turn and mid-points in Figure 4 survey pattern, plus first center pass, at four locations in primary eyewall. Also release dropsonde at ~50 nm spacing along circumnavigation in moat region. If Coyote is available, deploy it following the inflow path where it will collect observations that can be used to calculate BL characteristics outside, within, and inside outer eyewall. For G-IV, release dropsondes at all turn points.
- Pattern: For P-3, fly a combination of a rotated Figure-4 and a circumnavigation in the moat region, within ~5-10 nm of the inner edge of the outer eyewall. Fly the circumnavigation straight and level as long as possible, i.e., keeping aircraft bank angle at a minimum, to minimize loss of radar data due to aircraft banking. Ferry time may preclude the second Figure-4. For G-IV, fly pattern such that the innermost circumnavigation is as close to outer edge of outer eyewall as is safely allowed

Module Option 3 (PRE-SEF/ POST-SEF): When available, Global Hawk aircraft dropsondes can provide complementary observations compared to P-3 and G-IV (Fig. 18-3). Global Hawk flies at approximately 55,000-60,000 ft altitude with mission durations of ~24 hour. It will provide excellet temporal coverage that might be critical to analyze the evolution of the secondary eyewall.

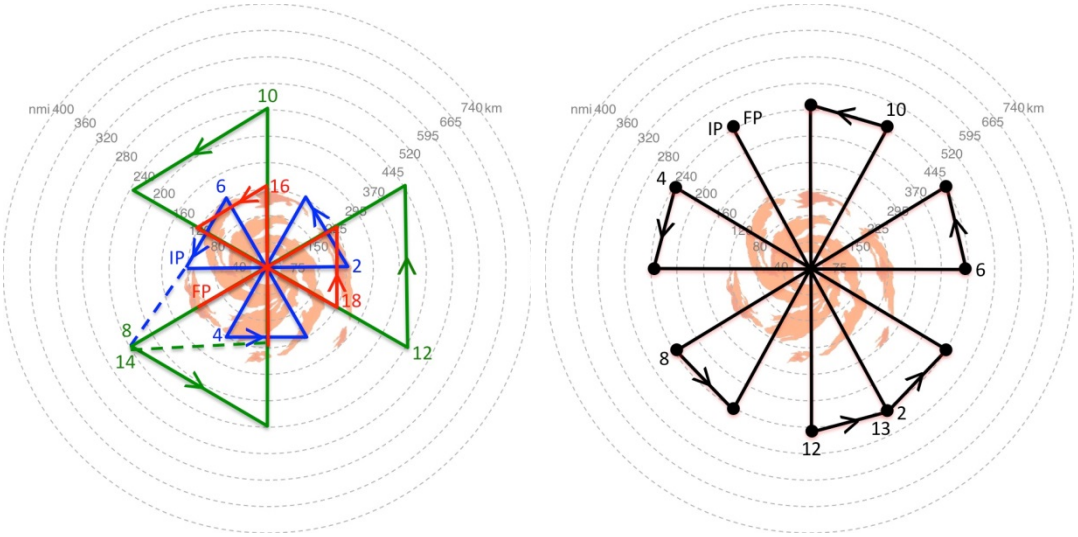

Figure 18-3*: Sample flight patterns for the NOAA SHOUT Global Hawk aircraft. (Left) Series of 3 alternating radial leg butterfly patterns shown by the green line and (right) rotated butterfly pattern with 30 degree rotated radial legs. On-station time for both patterns is ~15-20 hr and leg lengths are ~450 km.*

- Altitude: 55-60,000 ft
- Expendables: Deploy dropsondes at all turn points, RMW, 2*RMW. If the storm shows one concentric ring, left flight pattern preferable. Deploy dropwonds at the eye, first eyewall, secondary eyewall (if shown), and all turn points. If only one primary rainband with no clear-defined eye, perform right flight pattern.
- Instrumentation: Dropsondes.

Analysis Strategy:

Data collected by option 1 can be used to diagnose different roles in SEF. Specifically, gradient wind (and departures thereof) within and above the BL can be calculated from dropsondes; tangential winds and vorticity can be calculated from dropsonde, Doppler radar, flight-level, and DWL measurements; and moist static energy calculation, can be calculated from dropsondes. Observations that are collected can also be used to conduct data impact studies as well as provide insights for OSSE studies.

Data measured by option 2 would be useful to diagnose the formation and characteristics of the moat region and its role in ERC. Azimuthal coverage of the data would be particularly important to carry out analysis to validate different hypotheses of SEF/ERC. Data collected by module option 3 can provide longer temporal coverage than option 1 and 2 that will be useful to diagnose the temporal evolution of the SEF/ERC.

References:

Abarca, S. F., and K. L. Corbosiero, 2011: Secondary eyewall formation in WRF simulations of Hurricanes Rita and Katrina (2005). *Geophys. Res. Lett.*, **38**, 1-5.

Abarca, S. F., and M. T. Montgomery, 2013: Essential Dynamics of Secondary Eyewall Formation. *J. Atmos. Sci.*, **70**, 3216-3230.

Abarca, S. F., M. T. Montgomery, S. Braun, and J. Dunion, 2016: Secondary Eyewall Dynamics as Captured by an Unprecedented Array of GPS Dropsondes Deployed into Edouard 2014, 32nd Conf. on Hurricanes and Tropical Meteorology, San Juan, PR.

Bell, M. M., M. T. Montgomery, and W.-C. Lee, 2012: An Axisymmetric View of Concentric Eyewall Evolution in Hurricane Rita (2005). *J. Atmos. Sci.*, **69**, 2414-2432.

Corbosiero K. L., and R. D. Torn, 2016: Diagnosis of Secondary Eyewall Formation Mechanisms in Hurricane Igor (2010), 32nd Conf. on Hurricanes and Tropical Meteorology, San Juan, PR.

Didlake Jr., A. C., and R. A. Houze, 2011: Kinematics of the Secondary Eyewall Observed in Hurricane Rita (2005). *J. Atmos. Sci.*, **68**, 1620–1636.

Didlake, Jr., A. C., and R. A. Houze, 2013a: Convective-Scale Variations in the Inner-Core Rainbands of a Tropical Cyclone. *J. Atmos. Sci.,* 70, 504-523.

Didlake, A. C., and R. A. Houze, 2013b: Dynamics of the Stratiform Sector of a Tropical Cyclone Rainband. *J. Atmos. Sci.*, 70, 1891-1911.

Hawkins, J. D., and M. Helveston, 2008: Tropical cyclone multiple eyewall characteristics. Preprints, 28th Conf. on Hurricanes and Tropical Meteorology, Amer. Meteor. Soc., Orlando, FL.

Huang, Y.-H., M. T. Montgomery, and C.-C. Wu, 2012: Concentric Eyewall Formation in Typhoon Sinlaku (2008). Part II: Axisymmetric Dynamical Processes. *J. Atmos. Sci.*, 69, 662-674.

Judt, F., and S. S. Chen, 2010: Convectively Generated Potential Vorticity in Rainbands and Formation of the Secondary Eyewall in Hurricane Rita of 2005. *J. Atmos. Sci.*, 67, 3581-3599.

Kepert, J. D., 2013: How does the boundary layer contribute to eyewall replacement cycles in axisymmetric tropical cyclones? *J. Atmos. Sci.*, 70, 2808-2830.

Li, Q., Y. Wang, and Y. Duan, 2014: Effects of Diabatic Heating and Cooling in the Rapid Filamentation Zone on Structure and Intensity of a Simulated Tropical Cyclone. *J. Atmos. Sci.,* 71, 3144-3163.

Montgomery, M. T., and R. J. Kallenbach, 1997: A theory for vortex Rossby-waves and its application to spiral bands and intensity changes in hurricanes. *Quart. J. Roy. Meteor. Soc.,* 123, 435-465.

Moon, Y., and D. S. Nolan, 2010: The Dynamic Response of the Hurricane Wind Field to Spiral Rainband Heating. *J. Atmos. Sci.*, 67, 1779-1805.

Moon, Y., D. S. Nolan, and M. Iskandarani, 2010: On the Use of Two-Dimensional Incompressible Flow to Study Secondary Eyewall Formation in Tropical Cyclones. *J. Atmos. Sci.*, **67**, 3765-3773.

Rozoff, C. M., D. S. Nolan, J. P. Kossin, F. Zhang, and J. Fang, 2012: The Roles of an Expanding Wind Field and Inertial Stability in Tropical Cyclone Secondary Eyewall Formation. *J. Atmos. Sci.,* 69, 2621–2643.

Sitkowski, M., J. P. Kossin, and C. M. Rozoff, 2011: Intensity and Structure Changes during Hurricane Eyewall Replacement Cycles. *Mon. Wea. Rev.,* 139, 3829-3847.

Wang, Y., 2009: How Do Outer Spiral Rainbands Affect Tropical Cyclone Structure and Intensity?. *J. Atmos. Sci.*, 66, 1250-1273.

Wu, C.-C., Y.-H. Huang, and G.-Y. Lien, 2012: Concentric Eyewall Formation in Typhoon Sinlaku (2008). Part I: Assimilation of T-PARC Data Based on the Ensemble Kalman Filter (EnKF). *Mon. Wea. Rev.*, 140, 506–527.

Zhu, Z.-D., and P. Zhu (2014), The role of outer rainband convection in governing the eyewall replacement cycle in numerical simulations of tropical cyclones*, J. Geophys. Res. Atmos*., 119, 8049–8072